FATIGUE CRACK GROWTH. OVERLOAD AND UNDERLOAD INTERACTIONS

P. Yasniy, Yu. Pyndus, V. Fostyk, I. Shulgan

Ternopil Ivan Pul'uj State Technical University, Ukraine

Abstract. This article deals with the study of the overload- underload interactions effects on fatigue crack growth (FCG) rate. With the purpose of understanding of overload-underload interaction mechanisms the FEM modeling of stress-strain state at the crack tip was investigated. FCG tests with single tensile peak overloads and complex overloads- underloads have been performed in D16chT (analogue of American 2024 T3) aluminium alloy. Using the assumption of the principal role of residual stresses (as a result of plastic strain at crack tip) in crack growth retardation and acceleration, the FCG interaction model was developed. Based on the proposed FCG interaction model shows good correlation with calculated and experimental data.

Keywords: fatigue crack growth, overload, underload, retardation, residual stresses

Introduction

Fatigue design of machines and mechanisms components is a difficult and important task. The aims of fatigue evaluation of machines are to establish that catastrophic failure from fatigue is impossible within the service life and, additionally, to provide non-catastrophic exploitation of machine structure with cracks to enable economic utilization. These aims have to be achieved within the framework of minimum weight and cost, and maximum performance.

A common feature of most real load spectra is the presence of overloads and underloads.

The airplane wing loading spectra is the good example of such loadings. The influence of overloads, underloads and stress ratio variations on the fatigue life of a structure has been shown to be of key importance.

There are several main mechanisms which are used for explanation of overload and underload effects on FCG [1-8]:

- crack closure, induced by plasticity;
- residual stresses at crack tip;
- material hardening at crack tip;
- crack surface roughness;
- crack tip blunting.

In general case FCG retardation after single overload causes all mentioned mechanisms. But depending of load conditions (overload factor, stress ratio, stress range of regular loading, environment) and mechanical properties one or another mechanism can be dominated. For instance, crack closure and residual compressive stress, induced by plasticity at the crack tip are the principals crack growth retardation mechanism in D16chT aluminium alloy after overload [9].

Models of Wheeler and Willenborg were widely used for the explanation and prediction of FCG retardation after single overload and random loading [10, 12]. These models are based on the assumption about principal effect of residual compressive stresses at the crack tip on FCG retardation. The model of FCG after overload [13-15] implicitly takes into account all mechanism of crack growth retardation (residual stresses, material strain hardening, crack closure, etc). This model based on the conception of plastic zones interaction by Wheeler and Willenborg and effective stress σ_{eff}.

It is a well-known fact that after compressive overload (underload) FCG rate increases [4, 5, 16, and 17]. The presence of the underload in spectrum loading of some machines cans significant decrease the structure lifetime.

For instance, the spectrum loading of the lower wing panel of a transport airplane includes a compressive overload caused of a land running [18]. In contrast to tension overload the influence mechanisms of compressive overload on FCG rate are not clearly understood. In particular the influence of overload and underload on FCG rate under regular loading was carried out by Makabe C., Purnowidodo A., McEvily A.J., Yang Z. [16, 17].

They have found out that FCG acceleration effect is greater when compressive overload is applied after tension overload as to the case when compressive overload is applied after regular loading. It was explained that compressive overload changes plastic strain direction, decreases compressive stress at the crack tip and increases crack tip opening displacement range.

The aim of this work is to study the tension and compressive overload effect on FCG in D16chT aluminium alloy, stress strain state at crack tip and develop approach to FCG rate after overload-underload.

Crack tip plastic zone kinetics study

The stress-strain state after overload and underload was assessed by using FEM program complex ANSYS MULTIPHISICS. The assessments were made under the conditions of plain stress state in elastic-plastic body, with the help of iteration calculation of strains growth and the redistribution of stresses at crack tip with the gradual increase of load. The option of multilinear kinematic hardening plasticity (von Mises) [20] was used for the description of material's behaviour. The Bauschinger effect was also taken into account. The model of central crack tension specimens was given the mechanical properties of aluminium alloy D16ChT (Fig. 1).

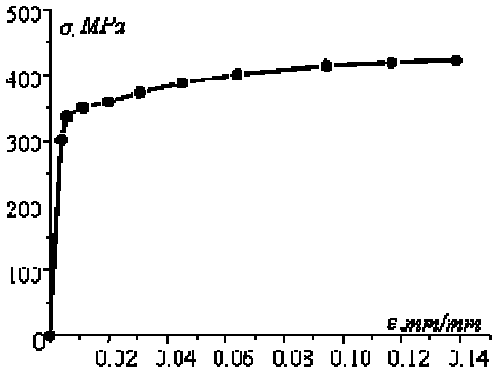

Figure 1. D16chT alloy stress-strain curve

Taking into account the symmetry of specimen only the half of it was used in the calculations. Two-dimensional (plain stress) quadrilateral-triangular finite element PLANE82 with 8 nodes was used for meshing [20]. The crack tip was meshed using singular (PLANE82) elements with the radius of first and second row equal to 0.2 mm and the number of elements around the crack tip equals to 16 (Fig. 2). The surfaces of crack were constrained as a contact pairs to prevent the crack surfaces penetration under compressive loading.

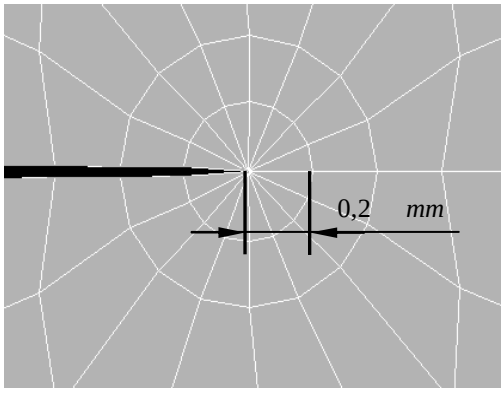

Figure 2. Singular elements around crack tip

It is a well-known that the overload factor is assessed as:

$$Q_{ol} = \sigma_{ol} / \sigma_{max} \qquad (1)$$

where σ_{ol} is overload stress, σ_{max} - maximal stress of regular loading cycle.

The interaction of overload and underloads is characterised by factor

$$Q_{ol} = \sigma_{ul} / \sigma_{ol} \qquad (2)$$

where σ_{ul} is underload stress.

The overload-underload scheme and the values of stresses in specimen are shown at the Fig. 3 and are given at the table 1.

The overload and underload stresses were obtained from the real operating sequence of plane

AN-140 (ANTONOV) wing. During the experiments and the FEM modelling the overload stress value within the selected series was constant while the value of underload stress has changed, as it is showed in table 1.

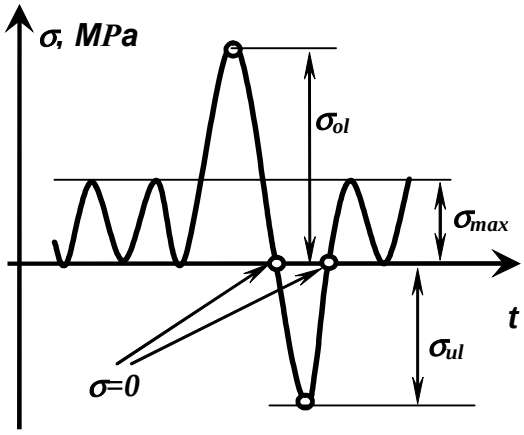

Figure 3. The overload-underload scheme

Table 1

Overload and underload stresses

σ_{ol} , MPa	σ_{ul} , MPa	Q_{ul}
161,2	-207,80	-1,3
	-161,20	-1
	-128,96	-0,8
	-96,70	-0,6
	-64,48	-0,4
145,42	-190,00	-1,3
	-170,00	-1,17
	-87,25	-0,6
120,47	-170,00	-1,41
	-120,47	-1
	-72,28	-0,6

For the quality assessment of overload and underload effect on the plastic zone (PZ) at crack tip, lets consider the case of overload at Q_{ul}=(-207.8)/161.2=(-1.3). Analysing the distribution of normal stresses σ_y in crack tip (Fig. 4), the following conclusions can be obtained:

- under the stresses equal to σ_{ol} =161.2, σ_y stresses are greater than the yield strength under the uniaxial load at the significant distance from crack's tip (Fig. 4, curve 1);
- after the unloading ($\sigma=0$), at some distance from the crack tip ($l \approx 3.5mm$) the significant compressive stresses are detected. It can be assumed as the main reason of FCG retardation after the overload (Fig. 4, curve 2);
- under the underload stress σ_{ul}=*-207.76* MPa, the increase of compressive σ_y stresses takes place at the distance *l>1.5* mm from the crack tip in comparison with the residual stresses at the specimen after previous unloading. The stresses at front of crack tip are greater than the yield strength of material, that points on the possible processes of backward material deformation within of primary PZ(Fig. 4, curve 3);
- after the following complete specimen unloading the tension residual stresses appear at the crack tip front at *l<1.0* mm and the residual stresses (*1.0* mm<*l*<*2.5* mm) are becoming significantly less than they were after overload (Fig. 4, curve 4).

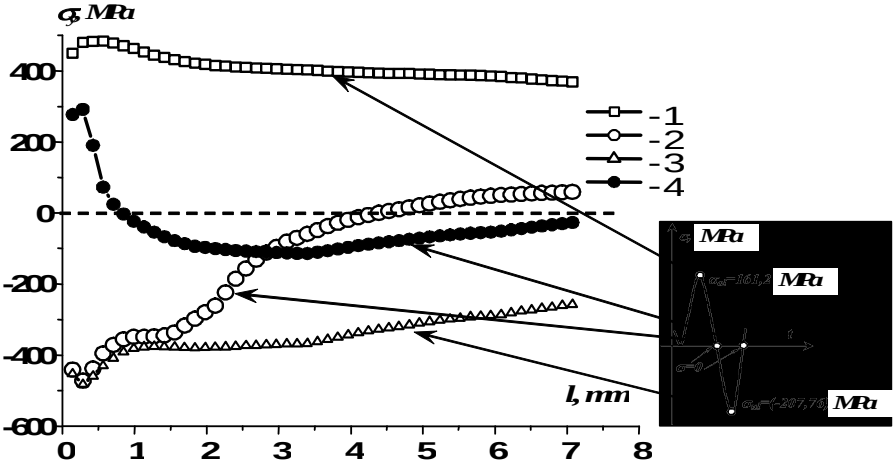

Figure 4. Distribution of normal stresses σ_y ahead of crack tip under the loading steps:
1 – σ_{ol} ***=161.2 MPa,*** 2 – ***σ=0 MPa,*** 3 – σ_{ul} ***=(-207.76) MPa ,*** 4 – ***σ=0 MPa***

Figure 5 shows the residual strains distributions ahead of a crack tip ε_y after the overload and following underload. One can see that the maximal residual strain was decreased after the underload ε_{ul} in comparison with the same values after tensile overload ε_{ol}. The PZ width l_{Kul} after underload also decreases in comparison with PZ width l_{Kol} after tensile overload.

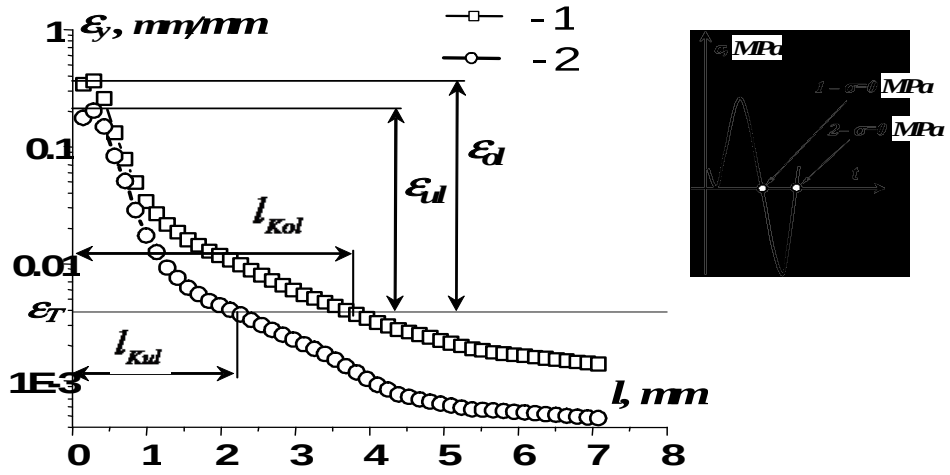

Figure 5. Residual strains (normal) ε_y after the overload (1) and underload (2)

For the estimation of overload-underload interactions on the PZ kinetics, the PZ width decreasing factor

$$k_l^{ul} = l_{Kul} / l_{Kol} \tag{3}$$

and the residual strain decrease factor

$$k_\varepsilon^{ul} = \varepsilon_{ul} / \varepsilon_{ol} \tag{4}$$

were proposed.

The influence of underload factor Q_{ul} on the k_l^{ul} and k_ε^{ul} values were carried out in accordance with the loading scheme and values of stresses presented on figure 3 and at table 1.

The factor k_l^{ul}, as well as the width of PZ is decreasing with the increasing of absolute value of underload stress (Fig. 6). This dependency becomes more significance with the increase of overload stress.

The change of residual strain decrease factor k_ε^{ul} versus underload factor Q_{ul} occurs with the same way as the change of k_l^{ul} (Fig. 7).

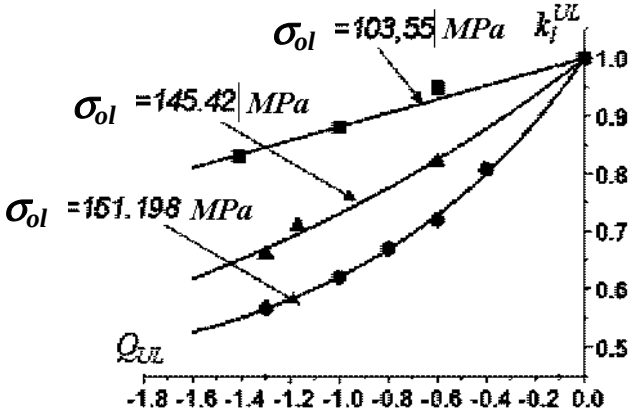

Figure 6. The dependences factor k_l^{ul} on Q_{ul}

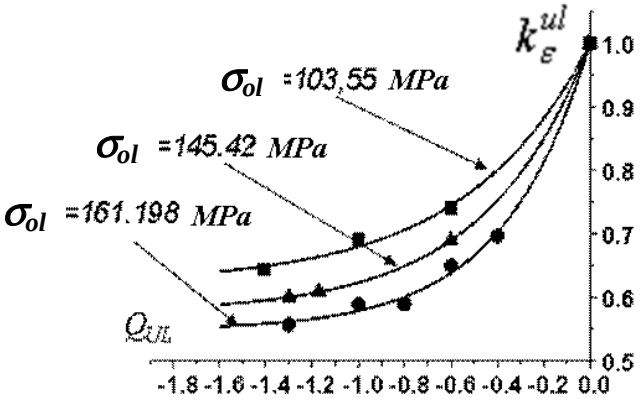

Figure 7. The dependences factor k_ε^{ul} on Q_{ul}

Thus, by using FEM it was found out, that the tension overload leads to the reduction of PZ width and relaxation of residual compressive stresses, which appear after the preliminary overload.

Hence the strain state after underload could be characterised with the PZ width decreasing factor k_l^{ul} and the residual strain decrease factor k_ε^{ul}.

FCG model after overload-underload

The FCG model after overload-underload is based on the FCG model after single overload [13-15] and FEM analysis of PZ at the crack tip. In this model (Fig.8) the influence of underload on FCG takes into account the PZ width decreasing factor k_l^{ul} (Eqn.8) and the residual strain decrease factor k_ε^{u}, (Eqns.10 and 13).

For the calculation of FCG rate after overload and underload the modified Walker equation is used [14]

$$V = C_R(K_{\max}^{eff}(1-R))^n, \qquad C_R = C_0\frac{1}{(1-R)^{(1-m)n}}, \tag{5}$$

where C_0, n are FCG material constants under regular loading, m is Walker's stress ratio layer factor.

The effective SIF $K_{\max}^{eff}$ is calculated using the well-known equation

$$K_{\max}^{eff} = \sigma_{eff}\sqrt{\pi l}\times Y, \qquad \sigma_{eff} = \sigma_{\max} - \sigma_{\text{int}}, \tag{6}$$

where σ_{int} is the residual stresses (Fig.8(b, c)), that are determined using the following equations

$$\begin{cases} \sigma_{\text{int}} = \sigma_{\text{int}}^{\max} - \dfrac{\sigma_{\text{int}}^{\max}}{(l_{K_{V\min}})^{\alpha_1}}\cdot(l_{K_{V\min}} - (l-l_0))^{\alpha_1}, & (l-l_0) < l_{K_{V\min}} \\ \sigma_{\text{int}} = \sigma_{\text{int}}^{\max} - \dfrac{\sigma_{\text{int}}^{\max}}{(l_{stab} - l_{K_{V\min}})^{\alpha_2}}\cdot((l-l_0) - l_{K_{V\min}})^{\alpha_2}, & (l-l_0) > l_{K_{V\min}} \end{cases}. \tag{7}$$

The equations (7) is the parabola (Fig.8 (b)) with the extreme at the point (l-l_0=l_{KVmin}, σ_{int} =σ_{int}^{max}). It begins at the point of overload with coordinates (l - l_0=0, σ_{int} = 0) and finishes at the point (l - l_0=l_{stab}, σ_{int} =0), when the FCG rate is considered to be stabilised. Equations (7) determines the distribution of residual stresses in the specimen that causes the FCG retardation after the single overloads.

According to model (Fig.8) at the equations (7) σ_{int}^{max} is maximal residual stress that is determined in respect to minimal FCG rate after the overload V_{min} [9, 19]. For calculate of the maximum residual stress σ_{int}^{max} (Eqn. 8) the residual strain decrease factor k_ε^{ul} was used. In conditions of underload, the absolute value of σ_{int}^{max} is decreasing, taking into consideration the factor k_ε^{ul}

$$\sigma_{\text{int}}^{\max} = \left[\sigma_{\max} - \frac{\sqrt[n]{V_{\min}/C}}{\sqrt{\pi l}Y(1-R)}\right]\times k_\varepsilon^{ul}, \tag{8}$$

where V_{min} is the minimal FCG rate after single overload that is calculated using the following equation :

$$V_{\min} = C_R(K_{\max}(1-R))^n g_R^{(Q_{ol}-1)}; \tag{9}$$

In the Equations (7)

l_0 is half crack length at the point of overload;

l_{stab} is the width of stabilisation zone of FCG rate (Fig.8(a,b))

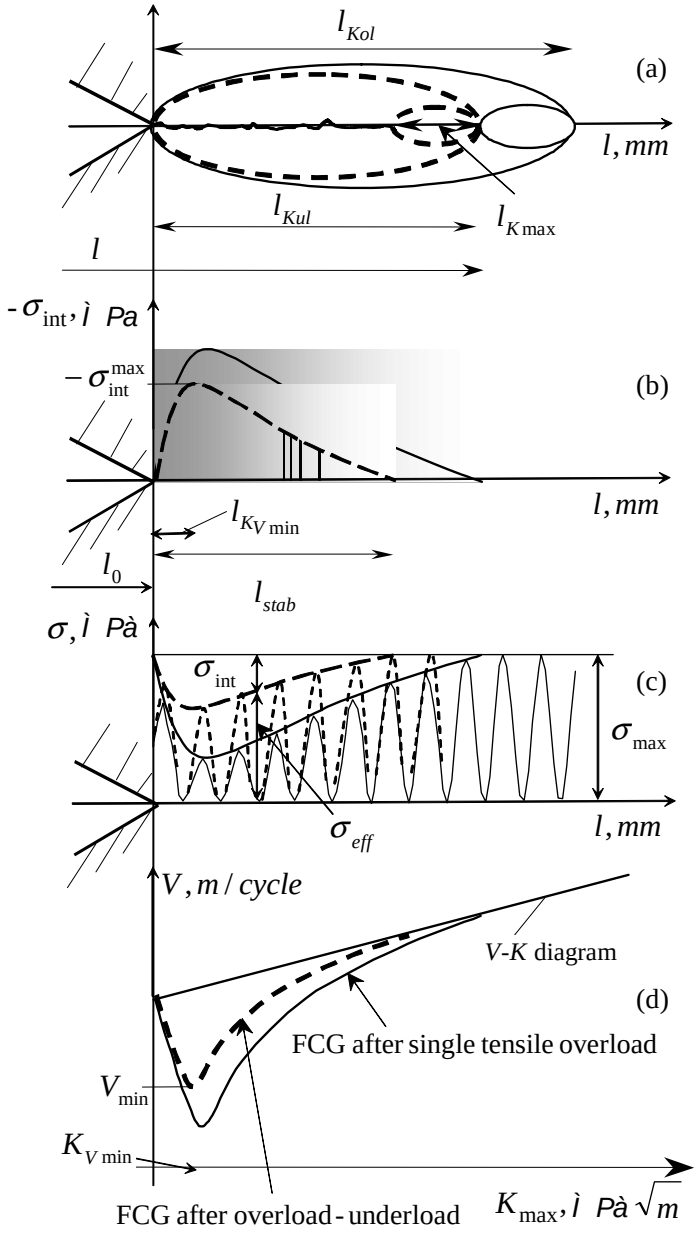

Figure 8. The model of FCG rate after single overload

$$l_{stab} = l_{Kol} \times k_l^{ul} - l_{K\max}, \quad (10)$$

where l_{Kol} is PZ width after overload; $l_{K\max}$ is PZ width under constant amplitude loading.

The PZ width l_{PZ}, $l_{K\max}$ and l_{Kol} for the plain stress state is determined using the equation

$$l_{PZ} = \frac{1}{\alpha\pi} \cdot \left(\frac{K_{APL}}{\sigma_{0,2}} \right)^2, \quad (11)$$

where $\sigma_{0,2}$ *is yield strength*; K_{APL} is applied SIF: K_{max} or K_{ol}; α=1 – the constant; $l_{K_{V\min}}$ is the distance from the point of overload to the point, at which the FCG rate is minimal. It was obtained experimentally, (for D16chT alloy)

$$l_{K_{V\min}} = \beta\, l_{Kol}, \quad (12)$$

where β=0,087 – the factor, that is determined as the mean experimental value for all cases of overload. Taking into account the PZ width decrease factor

$$l_{K_{V\min}} = \beta\, l_{Kol}\, k_l^{ul}. \quad (13)$$

Factors α_1 and α_2 in equation (7) determine the change of σ_{int} along the residual stresses zone width [13-15].

FCG after overload and underload: experiments and prediction

The FCG rate after the overload and underload was investigated on the servohydravlic testing machine STM-100 controlled by a PC. The center cracked tension specimens with the width W=100 mm, length L=300 mm and thickness B=3 mm were machined from the D16chT alloy (σ_B = 300 MPa, $\sigma_{0,2}$ = 430 MPa). Specimens were subjected to the cyclic loading with the stress ratio R = 0, frequency f =10 Hz and temperature 20° C.

For the estimation of effects of single overload and underload on the FCG rate were used the following schemes:

- single overload with SIF K_{ol} = 31.57 MPa√m under the regular load with K_{max} = 15.78 MPa√m (Fig. 9, 10, curve 1);
- single overload with SIF K_{ol} = 33.00 MPa√m, then the single underload K_{ul} = - 31.90 MPa√m under the regular loading with K_{max} = 16.40 MPa√m (Fig. 9, curve 2);

- single overload with SIF K_{ol} = 30.79 MPa√m, then, after fatigue crack extension on 1 mm, single underload K_{ul}=-30.65 MPa√m under the regular loading with K_{max} = 15.47 MPa√m (Fig. 9, curve 3).

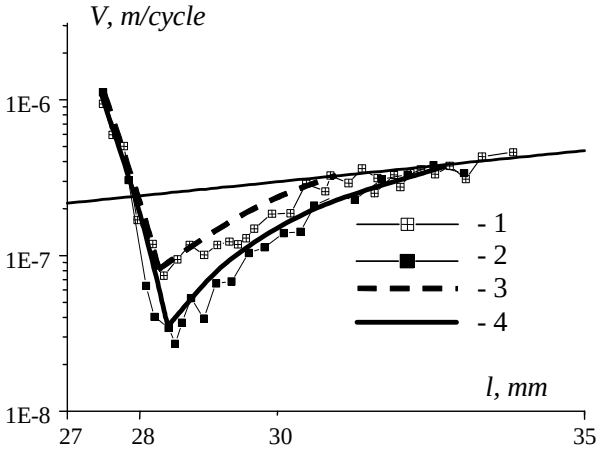

Figure 9. The FCG rate after:
1 – single overload at K_{max} = 15.78 MPa√m, K_{ol} = 31. MPa√m;
2 – overload-underload at K_{max} = 16.40 MPa√m, K_{ol} =33 MPa√m, Kul=-31.90 MPa√m.
3 – overload-underload (calculation);
4 – single overload (calculation)

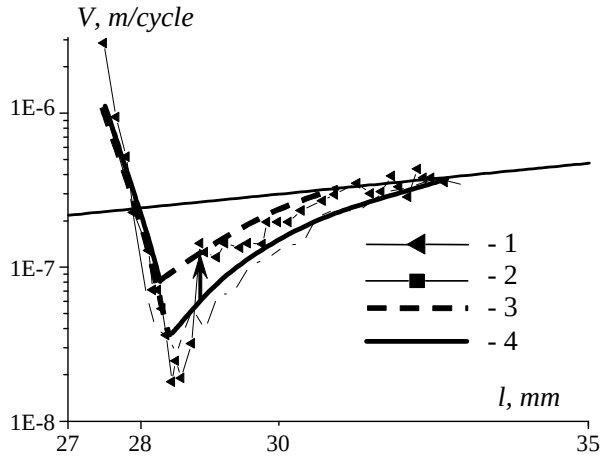

Figure 10. The FCG rate after:
1 – single overload at K_{max} = 15.78 MPa√m and K_{ol} = 31. MPa√m (experiment);
2 – overload at K_{max} = 15,47 MPa√m, K_{ol} =33,00 MPa√m and underload after 1 mm of crack extension at K_{ul}=-30.65 MPa√m (experiment);
3 – overload-underload (calculation);
4 – single overload (calculation)

The prediction of FCG rate after: overload; overload-underload; overload, fatigue crack extension on 1 mm and underload were done by the method of cycle-by-cycle calculation of crack growth with usage of proposed model.

It is obvious that the underload, applied after the overload causes the significant increase of FCG rate. The results of assessments are agreed well enough with experimental data.

The experimental data of FCG rate after overload (Fig. 10, curve 1), at first agreed with assessed curve 3, that describes single overload. After the underload, at the distance 1 mm from the point of overload, the experimental FCG rate (curve 2) is increased sharply and can be satisfactorily describe curve 4.

Thus, it can be assumed that the underload, that is applied after the crack extension (1 mm) within overload PZ, gives the same effect as the complex overload-underload. It is obvious, that the proposed model of FCG after overload-underload can be used for the prediction of FCG under random (tensile-compressive) loading.

Conclusions

1. The underload decreases the size of PZ in front of crack tip and residual stress that were created by the preliminary overload.
2. The FCG model after overload-underload was proposed. This approach is based on the analysis of stress- strain state at the crack tip, the PZ width and on the FCG rate data under regular loading.
3. The satisfactory correspondence between experimental and calculated data of FCG rate for different overload and overload schemes were obtained.

References

1. S. Suresh. Micromechanisms of fatigue crack growth retardation following overloads // Eng. Fract. Mech. – 1983. - Vol18. - 577–593.
2. Злочевский А.Б., Шувалов А.Н. Факторы тормозящие рост усталостных трещин после перегрузок // Физ.-хим. механика материалов. - 1985. - №2. – С.41-46.
3. Количественная фрактография. Усталостное разрушение / Иванова В.С., Шанявский А.А. – Челябинск: Металлургия, 1988. – 400 с.
4. Skorupa M. Load interaction effects during fatigue crack growth under variable amplitude loading – A litterature review. Part I : Empirical trends : Fatigue and Fracture of Engineering materials and structures. 1998, (21), 987-1006.
5. Skorupa M. Load interaction effects during fatigue crack growth under variable amplitude loading – A litterature review. Part II : Qualitative interpretation: Fatigue and Fracture of Engineering materials and structures, 1999, (22). 905-926.
6. K. Sadananda, A.K. Vasudevan, R.L. Holtz, E.U. Lee. Analysis of overload effects and related phenomena // Int. J. of Fatigue: Elsevier, 1999. - Vol.21. - P. 233-246.
7. J.C. Newman, Jr. A crack-closure model for predicting fatigue crack growth under Aircraft spectrum loading // Methods and models for predicting fatigue crack growth under random loading. - Philadelphia(Pa): ASTM STP No748, 1981, P. 53-84.
8. N.A. Fleek. Influence of stress state on crack growth retardation // Basic questions in fatigue. - Philadelphia(Pa): ASTM STP No924, 1988, P. 157-183.
9. P.V. Yasniy, Yu.I. Pyndus, O.I. Semenets. Influence of overloading on fatigue crack growth at various stress ratios// Visnyk of the Ternopil State Technical University.—Ternopil, TSTU – 2001. – Vol.6, №4. P. 5-12. (in Ukrainian).
10. O.E. Wheeler. Spectrum loading and crack growth // Journal of basic engineering. – ASME. – 1972. – P. 181-186.
11. J.P. Gallagher. A generalized development of yield-zone models. – AFFDL-TM-74-28-FBR. – 1974.
12. Johnson W. S. Multi-Parameter Yield Zone Model for Predicting Spectrum Crack Growth // Methods and Models for Predicting Fatigue Crack Growth under Random Loading.- Philadelphia(Pa): ASTM STP No748, 1981, P. 85-102.
13. Yu.I. Pyndus, P.V. Yasniy. The model of fatigue crack growth after single overload// Visnyk of the Zytomyr engineering- technology institute.-2002.-№1.-P.28-36. (In Ukrainian).
14. P. Yasniy, Yu. Pyndus. Prediction of Fatigue Crack Growth Rate after Single Overload at Different Stress Ratios // Proceedings of the 14th Bienniel Conference on fracture – ECF14. – Vol.3. – P.609-616.
15. Yu.I. Pyndus. Prediction of fatigue crack growth at variable amplitude loading in aluminum alloy D16T// Visnyk of the Ternopil State Technical University.—Ternopil, TSTU – 2002. – Vol.7, №1. P. 11-19. (in Ukrainian).
16. McEvily AJ, Yang Z. The nature of the two opening levels following an overload in fatigue crack growth // Metallurgical Transactions. – 1990. - 21A: 2717–27.
17. Makabe, C., Purnowidodo, A., and McEvily, A. J., “Effects of Surface Deformation and Crack Closure on Fatigue Crack Propagation after Overloading and Underloading,” Int. J.Fatigue, Vol. 26, 2004, pp. 1341–1348.
18. J. B. De Ionge, D. Schutz, H. Lowak, I. Schijve. A standardized load sequence for flight simulation tests on aircraft wing structures // LBF – Bericht FB-106, NLR TR 73029U. – 1973. - P. 1-17.
19. P.V. Yasniy, Yu.I. Pyndus. Influence of single overload on fatigue crack growth in aluminum alloy D16chT// Physico-chemical mechanics of materials.-2002.-№2.-P.57-60. (in Ukrainian).
20. ANSYS 9.0, Users Guide.